Journal of Sound and Vibration (1998) **215**(1), 63–79
Article No. sv981608

THE TRANSMISSION OF VIBRATION THROUGH A COUPLED PERIODIC STRUCTURE

Y. K. Tso

Department of Defence, Aeronautical and Maritime Research Laboratory—DSTO, Fishermens Bend, Victoria 3207, *Australia*

AND

C. H. Hansen

Department of Mechanical Engineering, The University of Adelaide, South Australia 5005, *Australia*

(*Received* 7 *March* 1996, *and in final form* 24 *February* 1998)

Complex built-up structures often consist of structural elements of a periodic nature. Examples of these include plate or shell elements reinforced by stiffeners at regular intervals. This paper describes a theoretical method for evaluating the coupling loss factor (CLF) of a coupled periodic structure for use in the application of statistical energy analysis. The structure considered consists of a plate with periodic stiffeners coupled at right angles to a uniform plate and the method of travelling wave analysis was used for the investigation. An experimental program was conducted to verify the CLF of the structure. Results from the measurements of input power and vibrational energy were used in a numerical procedure to determine the internal loss factors and CLF. The experimental results show good agreement with theoretical predictions at low frequencies. However, some discrepancies between the theoretical and experimental results were observed at high frequencies, possibly due to the frequency dependent nature of the assumptions involved in the theoretical analysis.

1. INTRODUCTION

Periodic structures are used extensively in engineering constructions. Examples of these may be found in many engineering applications such as ship structures (e.g. decks, bulkheads and hull structures) where relatively lightweight uniform plates or shells are reinforced by the attachment of stiffeners at regular intervals. The study of wave transmission through periodic structures is an integral part in the overall investigation of noise and vibration transmission through complex built-up structures such as ships and aircraft.

Brillouin [1] studied the wave motion of a number of periodic systems such as atoms, crystals and transmission lines using the Bloch (or Floquet) theorem. This approach greatly simplifies the analysis by relating the wave solutions in adjacent bays of the system. For a periodically supported beam of infinite extent in bending motion, the Bloch theorem gives the spatial variation of transverse displacement through each bay of the structure as [2]:

$$w(x + l) \exp(j\omega t) = \exp(\lambda) w(x) \exp(j\omega t), \tag{1}$$

0022–460X/98/310063 + 17 $30.00/0

where l is the length of an element in the periodic structure and λ is the propagation constant. If the propagation constant is purely imaginary, the bending wave will travel freely in the periodic structure. The frequency band in which wave propagation occurs is referred to as the pass band. On the other hand, if the propagation constant contains a real component, the bending wave will behave in an evanescent manner and the corresponding frequency band is referred to as the stop band.

The wave transmission properties of a large number of periodic structures (e.g. beams, plates and shells) have been studied extensively (see, for example, references [2–6]). However, periodic structures are often coupled to other structural elements to form complex built-up structures and the transmission of vibration through such complex structures has received less attention. Keane and Price [7] studied a one-dimensional coupled periodic structure using an enhanced statistical energy analysis (SEA) model which allows for the effects of pass and stop bands. These authors investigated a point spring coupled, multi-modal system and compared the results obtained from 'exact' modal analysis with the normal and enhanced SEA models. A significant improvement in results was obtained by using the enhanced SEA model rather than the normal model. However, the model studied by these authors was made up of idealised one-dimensional elements and therefore the analysis may not be readily applicable to engineering structures such as hull plates and bulkheads. The purpose of this paper is to investigate, both theoretically and experimentally, the transmission of vibration through a simple but practical engineering structure which consists of a periodic structural element. The structure considered in this paper is a plate with periodic stiffeners coupled at right angles to a uniform plate and the methods of travelling wave analysis and SEA are used in the theoretical investigation.

2. WAVE TRANSMISSION THROUGH A PLATE WITH PERIODIC STIFFENERS

A periodic structure which consists of stiffening beams attached symmetrically to both sides of a plate is chosen for the analysis (see Figure 1). This arrangement avoids the generation of in-plane waves in the plate-beam junction. The bending wave displacement of the plate may be obtained in a similar way as was done by Mead [2] in his treatment of a periodically supported beam, except that in this case the bending wave number has components in both the x- and y-directions due to the nature of the oblique wave. A detailed analysis of the plate with periodic stiffeners is given in the Appendix. This section outlines the procedures and results of the analysis.

For an arbitrary bay n ($n = 0, 1, 2, 3, \ldots, \infty$), the out-of-plane plate displacement is given by:

$$w(x_n) = \exp(\lambda n)\left\{\sum_{m=1}^{4} A_m \exp(k_{mx} x_n)\right\} \exp(k_y y + \mathrm{j}\omega t), \tag{2}$$

where l is the stiffener spacing, $x_n = x - nl$, k_{mx} is the root of the dispersion equaion for plate bending and A_m is the associated wave amplitude. The last exponential factor on the right-hand side of the above equation represents the y-direction dependency and time dependency of the wave amplitude.

By applying the compatibility and equilibrium conditions to two adjacent bays of the structure, the following matrix equation can be obtained (see Appendix):

$$\mathbf{\Lambda}[A_m] = \exp(\lambda)[A_m], \tag{3}$$

where $m = 1$–4, $\mathbf{\Lambda}$ is a 4×4 matrix defined by the system parameters and $[A_m]$ is a column vector representing the wave amplitudes.

Thus the analysis of wave propagation through a periodic structure may be reduced to a standard eigenvalue form. The four eigenvalues exist in two pairs, one of each pair being the reciprocal of the other, indicating the propagation of waves in both the positive and negative directions. The eigenvector which corresponds to each eigenvalue may be normalised to give $[1, A_2/A_1, A_3/A_1, A_4/A_1]^T$.

As an example, the propagation and attenuation zones of the plate with periodic stiffeners shown in Figure 1 were evaluated in terms of the wave heading angle and frequency. The plate and beam materials are steel with an elastic modulus of $1{\cdot}95 \times 10^{11}$ N/m^2, density of 7700 kg/m^3 and Poisson's ratio of 0·3. The thickness of the plate is 2 mm and the beams are 6×14 mm sections spaced at 100 mm apart. Figure 2 shows the propagation and attenuation zones of the structure. At normal incidence (zero wave heading angle), the first four stop bands lie within a frequency range of 359–483, 1535–1884, 3598–4048 and 6591–6730 Hz.

The wave transmission through two-dimensional elements such as a plate with periodic stiffeners differs from that through one-dimensional elements in that the former is dependent on the wave heading angle and frequency. Consider a plate with periodic stiffeners subjected to a diffuse vibration wave field. The incident wave will find a range of angles that transmit the wave freely and therefore two-dimensional elements do not normally exhibit a single pass or stop band at a particular frequency as is the case for one-dimensional periodic structures.

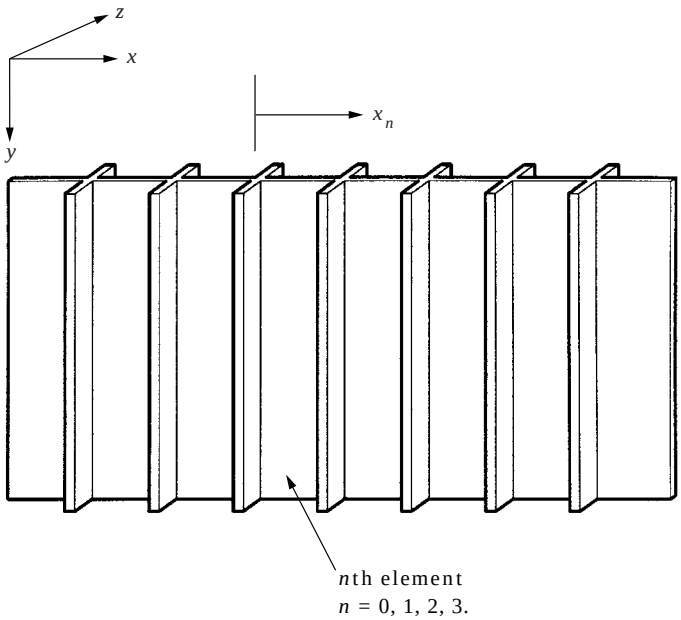

Figure 1. A plate with periodic beam stiffeners.

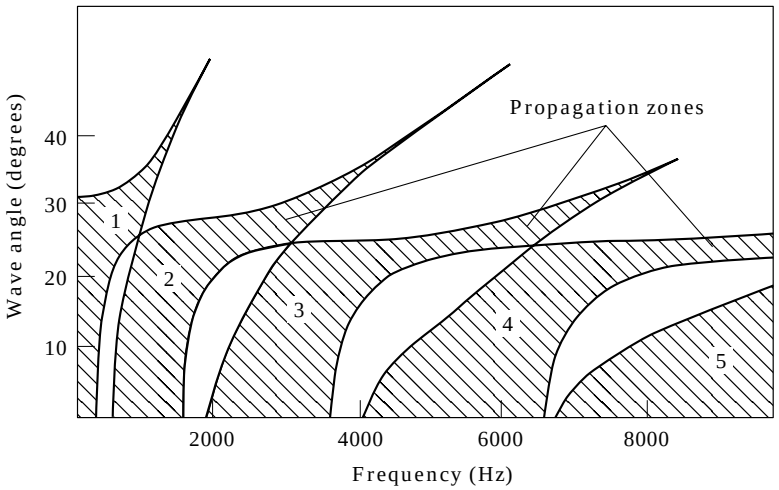

Figure 2. Propagation and attenuation zones of a plate with periodic stiffeners.

3. COUPLED PERIODIC STRUCTURE

3.1. ANALYSIS

Figure 3 shows a coupled periodic structure which consists of a plate with periodic stiffeners coupled at right angles to a uniform plate. Both plate elements are assumed to be of semi-infinite extent to avoid the complication of wave reflection at the plate edge boundaries. This particular structural junction is chosen on the basis of simplicity as well as its resemblance to many practical engineering structures including naval ship structures.

If the uniform plate is subjected to an incident bending wave, it will be partially transmitted and partially reflected as bending and in-plane waves. Cremer *et al*. [8] studied the wave transmission properties of structural junctions which consist of two uniform

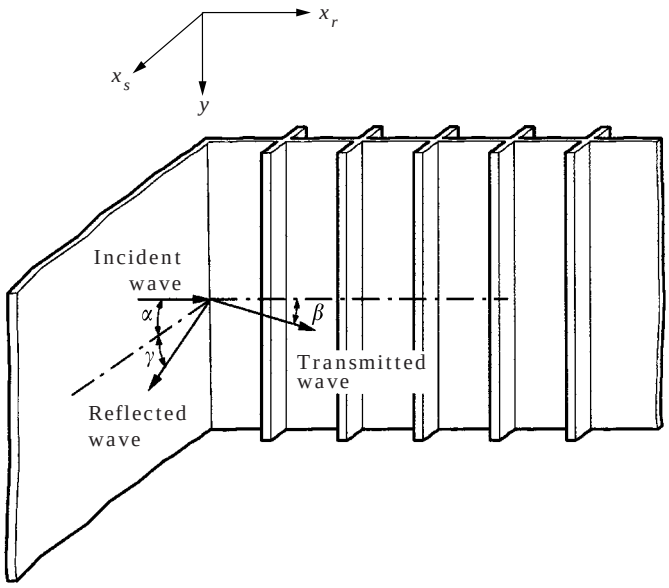

Figure 3. A coupled periodic structure.

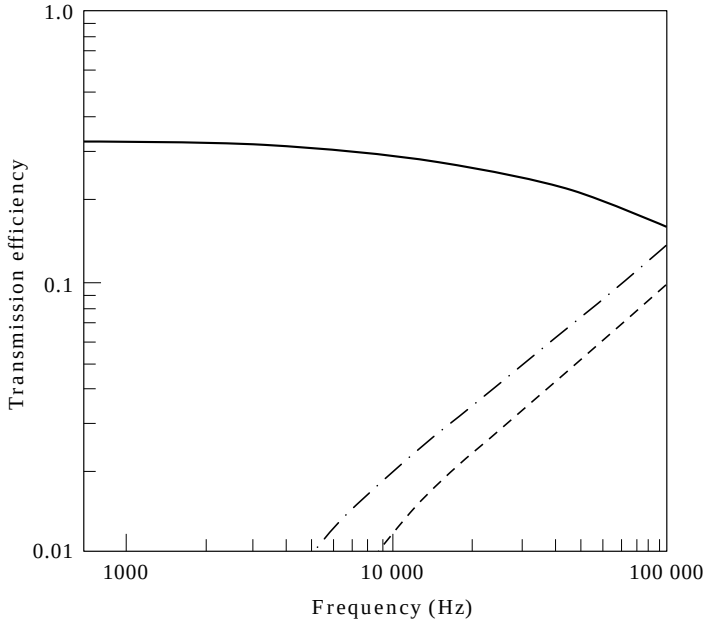

Figure 4. Transmission efficiency of a right-angled two plate junction subjected to an incident bending wave. ——, bending wave; — · —, shear wave; – – –, longitudinal wave.

plates coupled at right angles subjected to an incident bending wave. Their findings show that the power of the transmitted and reflected in-planes waves are negligible if the bending wave velocities of the plates are small compared with the in-plane wave velocities. In other words, the in-plane waves are negligible at low frequencies or for small plate thickness. As an example, the wave transmission efficiencies of a right-angled plate junction subjected to an incident bending wave were calculated (see, for example, reference [8] for details of the calculations) and shown in Figure 4. The junction consists of two uniform semi-infinite steel plates with the same thickness of 2 mm. It can be seen that the transmission efficiencies for the longitudinal and transverse shear waves are small compared with the bending wave up to a frequency of approx. 10 kHz.

The present analysis follows the assumption that the power of the in-plane waves are small compared with the bending wave. This assumption greatly simplifies the analysis and allows the band pass nature of the bending wave in a coupled periodic structure to be examined. However, it should be mentioned that with the preceding assumption, the present analysis is only valid for thin plates or low frequencies. The effect of in-plane waves in a periodic structure will be considered by the authors at a later stage.

Consider the uniform plate of the coupled period structure as the source plate which carries an oblique incident bending wave with a wave angle α (see Figure 3). The out-of-plane displacement for the source plate is given by [8]:

$$w_s = \{\exp(\mathrm{j}k_s x_s \cos\alpha) + B_1 \exp(-\mathrm{j}k_s x_s \cos\gamma) + B_2 \exp[-k_s x_s \sqrt{(1 + \sin^2\gamma)}]\}$$

$$\times \exp(k_{sy} y + \mathrm{j}\omega t), \tag{4}$$

where B_1 and B_2 are the complex wave amplitudes of the travelling and decaying reflected waves respectively, subscript s represents the source plate, and γ is the reflected bending wave angle which is related to the incident wave angle α through Snell's law.

For the plate with periodic stiffeners (the receiving plate), the out-of-plane displacement due to waves in the positive x-direction may be expressed in terms of two eigenvalues λ_1 and λ_2, together with their associated eigenvectors:

$$w_r = \left\{\exp(\lambda_1 n)\left[A_1 \sum_{m=1}^{4} (A_m/A_1)\exp(k_{mx}x_n)\right] + \exp(\lambda_2 n)\left[A_1' \sum_{m=1}^{4} (A_m'/A_1')\exp(k_{mx}x_n)\right]\right\}$$

$$\times \exp(k_y y + j\omega t), \tag{5}$$

where subscript r represents the receiving plate.

The expressions for plate displacements of the coupled structure therefore consist of four unknown wave amplitudes (B_1, B_2, A_1 and A_1'). With the assumption that the in-plane waves are negligible in the transmission of wave power, the boundary conditions at the junction may be approximately expressed in terms of the displacements, rotations and moments as shown below:

- the plate displacements at the junction are equal to zero,

$$w_s = 0, \tag{6}$$

$$w_r = 0, \tag{7}$$

- the plate rotations at the junction must be compatible,

$$\partial w_s/\partial x_s = \partial w_r/\partial x_r, \tag{8}$$

- the plate bending moments must be in equilibrium,

$$D_r[\partial^2 w_r/\partial x_r^2 + \mu_r\,\partial^2 w_r/\partial y^2] + D_s[\partial^2 w_s/\partial x_s^2 + \mu_s\,\partial^2 w_s/\partial y^2] = 0, \tag{9}$$

where D_r, D_s are the flexural rigidity of the receiving and source plates respectively, and μ_r, μ_s are the Poisson's ratios of the receiving and source plates respectively. Solution of the boundary conditions at the junction (i.e. $x_s = 0$, $n = 0$ and $x_r = 0$) leads to the four complex wave amplitudes and the wave powers may be expressed as:

$$\Pi = 1/2\ \mathrm{Re}\ \{M\dot{\phi}^*\}, \tag{10}$$

where $\cdot$ and * represent the derivative with respect to time and the complex conjugate respectively, M is the bending moment and ϕ is the plate rotation. The transmission efficiency is defined as the ratio between the transmitted wave power and the incident wave power, and is a function of the incident wave angle α. If one assumes that the source plate carries a diffuse vibration field, one may average the efficiency from an incident wave angle α of $-\pi/2$ to $\pi/2$ radians and obtain the mean transmission efficiency which is defined as [8]:

$$\tau = 1/2 \int_{-\pi/2}^{\pi/2} \tau(\alpha)\cos\alpha\ \mathrm{d}\alpha. \tag{11}$$

It should be noted that the transmission efficiency $\tau(\alpha)$ can only assume non-zero values at a range of wave angles which is governed by the propagation zones of the beam stiffened plate (see Figure 2) since wave transmission is not permitted in the attenuation zones. The coupling loss factor (CLF) between the uniform plate and the plate with periodic stiffeners may then be expressed as [8]:

$$\eta_{sr} = [c_{gs} l_c/(\pi\omega A_s)]\tau, \tag{12}$$

where c_{gs} is the group velocity of the uniform plate (the source plate), l_c is the coupling line length and A_s is the area of the uniform plate. Theoretical expressions for the modal density and group velocity of one- and two-dimensional periodic structures based on the propagation constant have been derived by Langley [9].

3.2. NUMERICAL EXAMPLE

The theory developed in the preceding sections was applied to a coupled periodic structure (see Figure 3) to illustrate the method of analysis. Only the transmission efficiency is considered in this section since it is independent of the plate area and may be regarded as a more general parameter (compared with the CLF) for characterising the wave transmission properties of the structure. Equation (12) may be used to evaluate the CLF if required. The plate with periodic stiffeners has the same parameters as for the example presented in Section 2 while the uniform steel plate has a thickness of 2 mm. Figure 5 shows the transmission efficiency as a function of the incident wave angle at a frequency of 1000 Hz. The incident angles that allow for free wave propagation are 0–26 degrees (propagation zone 2) and 30–36 degrees (propagation zone 1). The mean transmission efficiency of the coupled structure [equation (11)] was also evaluated as a function of

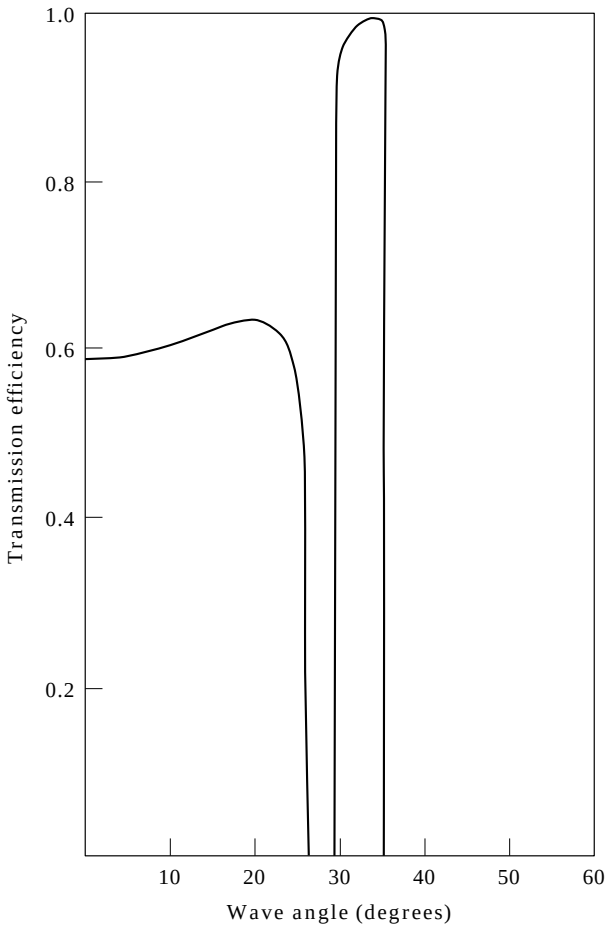

Figure 5. Transmission efficiency as a function of the incident wave angle for a uniform plate connected at right angles to a plate with periodic stiffeners.

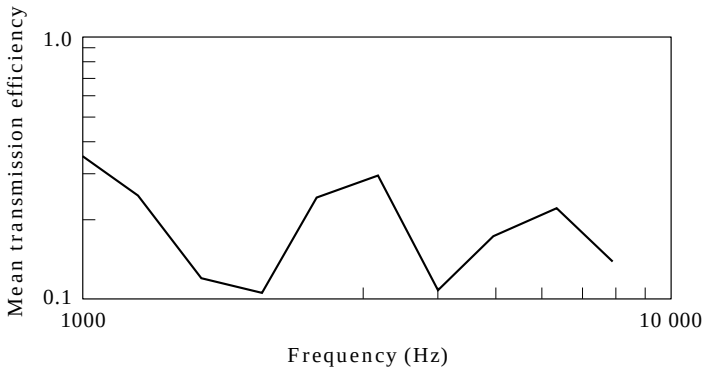

Figure 6. Mean transmission efficiency of a coupled periodic structure consisting of a uniform plate coupled to a plate with periodic stiffeners.

frequency and averaged in the one-third octave band as shown in Figure 6. A drop in the transmission efficiency can be observed at band centre frequencies of 1600, 2000 and 4000 Hz where the wave transmission properties are dominated by the attenuation zones. It is interesting to note that for two uniform plates of equal thickness coupled at a right angle, the mean transmission efficiency has a constant value (independent of frequency) of 0·333 [8].

4. EXPERIMENTAL INVESTIGATION

4.1. EXPERIMENTAL PROCEDURE

The preceding section suggests that the method of travelling wave analysis may be used for deriving the CLF, provided that the band pass nature of the plate with periodic stiffeners is accounted for in the evaluation of mean transmission efficiency. This section describes an experimental program to verify this assumption by measuring the CLF of a coupled periodic structure for comparison with theoretical predictions. The elements of the test structure consisted of a beam stiffened plate of 0·7 m $\times$ 1·2 m and a uniform plate of 0·7 m $\times$ 1 m. All the other system parameters were the same as for the example presented in Section 3.2. Mobility and steady state power balance measurements were conducted on the individual structural elements to determine their modal densities and internal loss factors respectively. The elements were then welded at right angles to each other and further tests conducted on the coupled structure to determine the input power and vibrational energy due to a random input excitation. A numerical procedure was used to evaluate the internal loss factor of the structural elements *in situ* as well as the CLF.

Consideration was given to the damping requirement for the structural elements. If the CLF of the coupled structure is very much greater than the internal loss factor of the individual elements, then the modal energy of the elements would be approximately equal (equipartition of energy) and insensitive to any variations in the CLF. To determine the CLF from energy and power measurements, it is therefore desirable to have the internal loss factors at least being of the same order of magnitude as that of the CLF. For the present study, this was achieved by adding self-adhesive damping strips to both plate elements. The added damping also increased the modal overlap of the structural elements to a level that enabled the travelling wave analysis procedure to be used for the determination of CLF [10].

Figure 7 shows the set up of the experiment for mobility and steady state power balance measurements. The structural element was suspended by strings and driven by a shaker through an impedance head. Six lightweight accelerometers located randomly on the structural element were used to determine the spatially-averaged mean square velocity and hence the vibrational energy. Subsequent to the joining of the beam stiffened plate to the uniform plate, measurements were carried out to determine the input power and the distribution of vibrational energy by first exciting the beam stiffened plate and then repeating the experiments by exciting the uniform plate. This arrangement provides the necessary experimental data so that checks can be made to determine if the experimental procedure satisfies the condition for reciprocity. The results for each set of measurements (i.e. mobility as well as the input power and the corresponding vibrational energy) were averaged over three randomly chosen excitation points.

To determine the mobility of the structure, the following expression which allows for a correction of the effect of seismic mass was used:

$$Y = (A_h/\mathrm{j}\omega)/(F_h - A_h m_s), \tag{13}$$

where Y is the drive point mobility, A_h and F_h are respectively the complex amplitudes of the acceleration and force signals from the impedance head, m_s is the seismic mass which includes the mass between the sensing element and the surface of the structure plus the associated mounting accessories.

Care was taken to minimise the force contact area by inserting a spacer of 5 mm diameter between the impedance head and the structure so that the results measured by the impedance head [equation (13)] may be regarded as the drive point mobility. For the present experiment, the structural wavelength at the highest one-third octave band (8000 Hz band centre frequency) was approximately ten times the diameter of the contact area; thus the attachment of the impedance head to the structure may be regarded as a point contact.

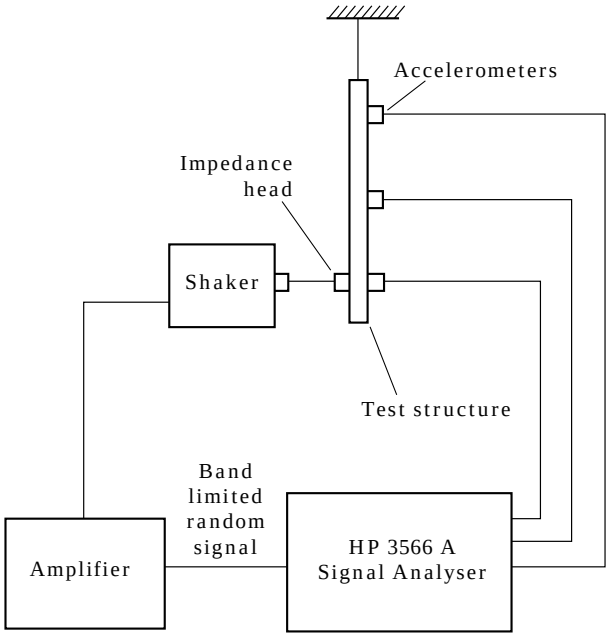

Figure 7. Experimental setup for mobility and steady state power balance measurements.

The modal density, $n(\omega)$, of the structural element was obtained from the drive point mobility as [8]:

$$n(\omega) = 1/(\omega_2 - \omega_1) \int_{\omega_1}^{\omega_2} 4m_e \,\mathrm{Re}\,(Y)\,\mathrm{d}\omega, \tag{14}$$

where m_e is the mass of the structural element.

To determine the power injected into the structural element, the force and acceleration signals from the impedance head were processed using the following relationship:

$$\Pi = 1/2\ \mathrm{Re}\,\{F_h \times (A_h/\mathrm{j}\omega)^*\}. \tag{15}$$

It should be noted that the seismic mass has no effect on the measurements of input power since it only results in an imaginary term. The vibrational energy of the structural element was obtained by averaging the signal from the accelerometers:

$$E = 1/2m_s\langle(A_s/\mathrm{j}\omega)^2\rangle_s, \tag{16}$$

where A_s is the complex amplitude of the signal from the accelerometers and $\langle\ \rangle_s$ denotes the spatial average.

The internal loss factor of the structural element was then determined from the input power, Π, and vibrational energy, E, as:

$$\eta = \Pi/\omega E. \tag{17}$$

A matrix inversion routine based on the minimisation of the sum of the squared errors [11] was used to determine the internal loss factors of the structural elements *in situ*, as well as the CLF of the coupled structure. This method involved a re-arrangement of the energy balance equations in the following form:

$$\Delta_1 = \eta_1 E_{11} + \eta_{12} E_{11} - \eta_{21} E_{21} - \Pi_1/\omega, \tag{18}$$

where E_{ij} is the energy of element i due to an input excitation at element j and Δ_1 denotes the experimental errors in determining the power and vibrational energy associated with subsystem 1. Similar equations may be formulated for other subsystems and for the present experimental set up, a total of four equations were formulated (two subsystems for each configuration of input excitation). The sum of the squared errors may then be expressed as:

$$\Gamma = \sum_{i=1}^{4} \Delta_i^2. \tag{19}$$

Following the least square procedure, the sum of the squared errors was minimised with respect to the internal loss factors and CLFs. It is convenient to generalise the internal loss factors and CLFs at this stage by denoting them as η_k. By using this notation, the expression for minimised error is given by:

$$\partial\Gamma/\partial\eta_k = 0. \tag{20}$$

The reciprocity condition [i.e. $n(\omega)_r\eta_{rs} = n(\omega)_s\eta_{sr}$] was incorporated into equation (20) and resulting in three linear algebraic equations (for $k = 1$, 2, and 3). The internal loss factors and CLF were then determined by standard matrix inversion of these equations.

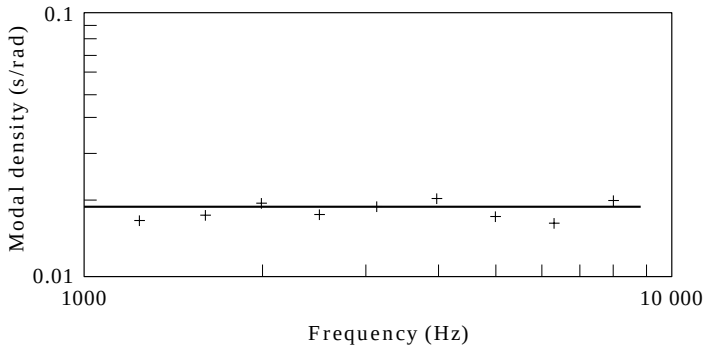

Figure 8. Modal density of uniform plate. ——, theory; +, measured.

4.2. RESULTS

The validity of the experimental procedure for measuring the modal density of the structural elements was checked by comparing the experimental results of the uniform plate with the following theoretical expression [12]:

$$n(\omega)_s = kA/(2\pi c_g), \tag{21}$$

where k is the wave number, A is the area of plate and c_g is the group velocity.

Figure 8 shows the modal density of the uniform plate. It can be seen that the measured modal density using the real part of the frequency-averaged drive point mobility [equation (14)] is in excellent agreement with the theoretical prediction, thus confirming the validity of the experimental procedure. The modal density of the plate with periodic stiffeners is shown in Figure 9. The results are somewhat higher than the sum of the modal densities for the plates and beams, possibly due to the effect of coupling which resulted in a shift of the natural frequencies.

Subsequent to the joining of the structural elements, measurements were carried out to determine the input power and the distribution of vibrational energy of the coupled structure. However, before using the numerical procedure to determine the CLF, the results were first checked for reciprocity. Clarkson and Rankine [13] have shown that the reciprocity requirement is satisfied when

$$[E_{rs}/\Pi_s n(\omega)_r]/[E_{sr}/\Pi_r n(\omega)_s] = 1. \tag{22}$$

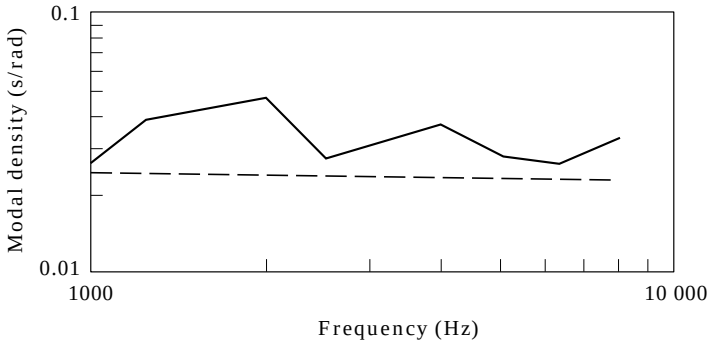

Figure 9. Modal density of plate with periodic stiffeners. ——, measured; — — —, sum of plate and beam modes.

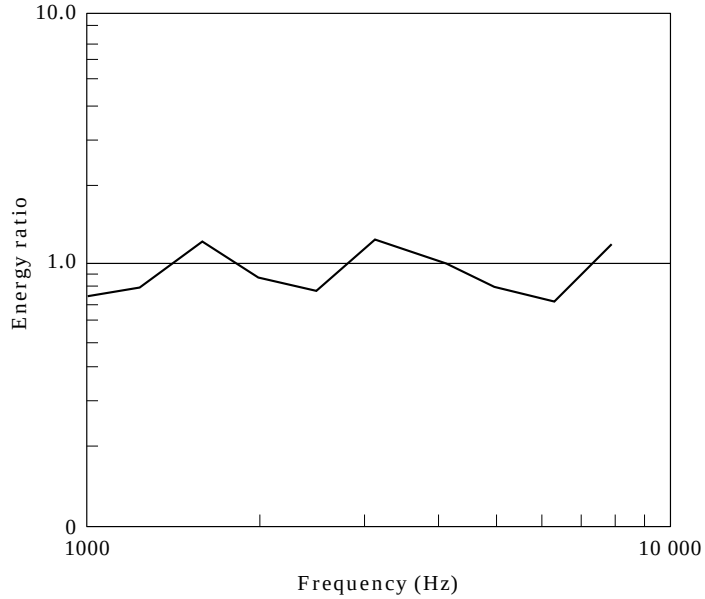

Figure 10. Energy ratio of the coupled periodic structure as a measure of reciprocity.

The left-hand side of equation (22) representing the energy ratio is plotted in Figure 10. It can be seen that the energy ratio is close to unity across the entire frequency range, thus the results satisfy the requirement for reciprocity.

The numerical procedure described in Section 4.1 was used to determine the internal loss factors *in situ* and the CLF. Figures 11 and 12 show the internal loss factors of the uniform plate and the plate with periodic stiffeners respectively. Results measured by both the *in*

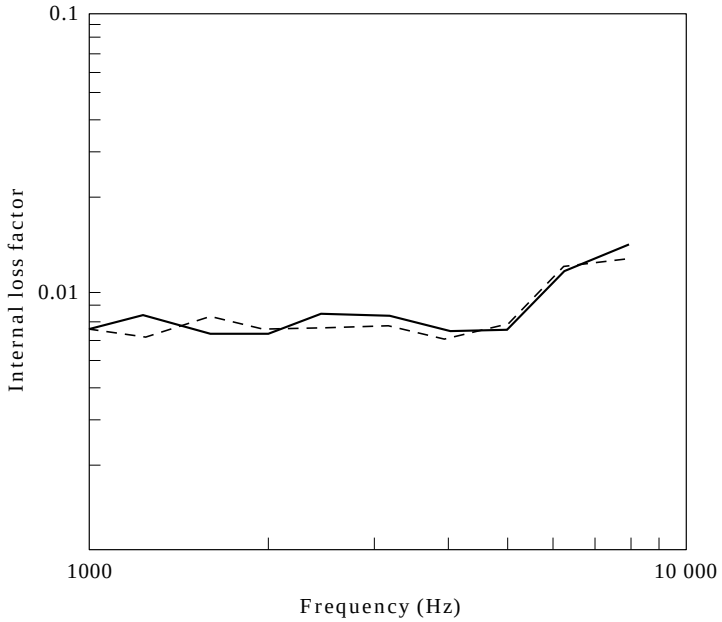

Figure 11. Internal loss factor of uniform plate. ——, Steady-state power balance method; — — —, *in situ*.

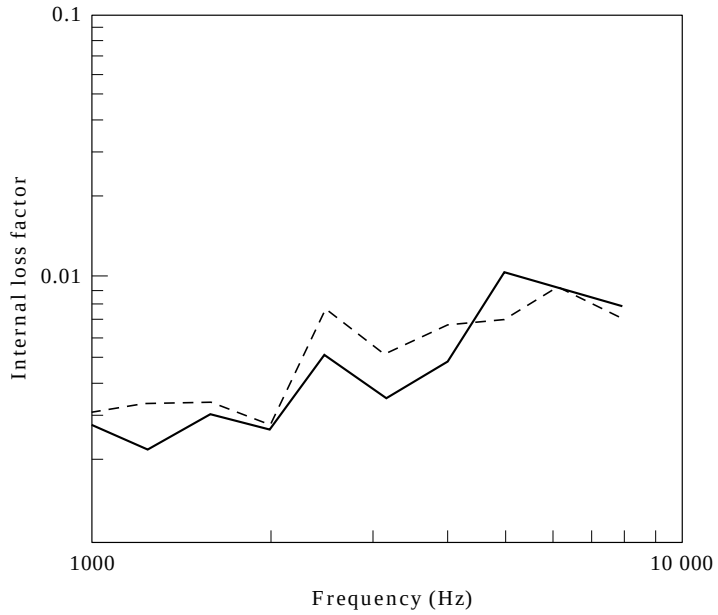

Figure 12. Internal loss factor of plate with periodic stiffeners. ——, Steady-state power balance method; — — —, *in situ*.

situ method and the steady state power balance method [equation (17)] are shown in the figures. It can be seen that these two methods of measurement are in close agreement and hence the results support the present experimental approach in determining the CLF.

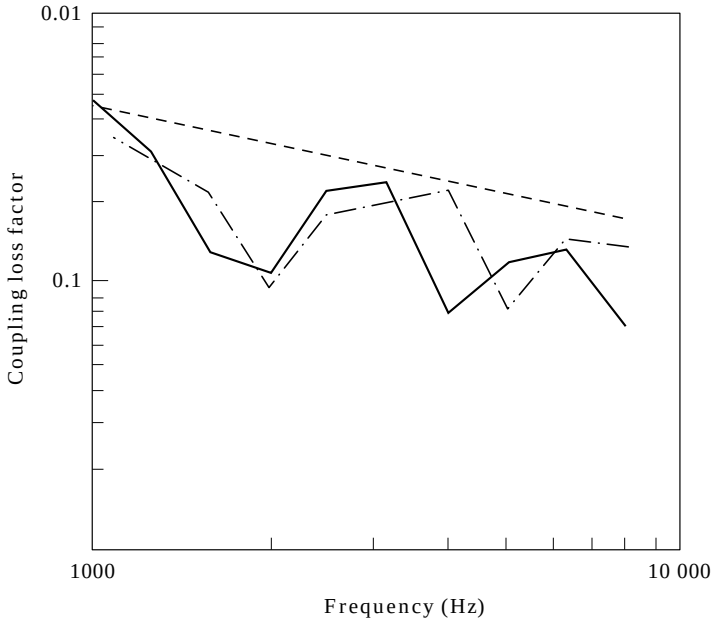

Figure 13. Coupling loss factor between a uniform plate and a plate with periodic stiffeners. ——, Theory; — · —, experiment; — — —, uniform plate/uniform plate.

Figure 13 shows the CLFs of the coupled periodic structure obtained by equation (12) and measurement. The results are in very good agreement in the lower frequency bands. At high frequencies, the theoretical results appear to have shifted by one-third of an octave compared with the experimental data. The apparent shift in frequency may have been caused by the assumptions and simplifications involved in the theoretical analysis. For example, it is assumed in the analysis that the boundary conditions of the plate with periodic stiffeners can be applied on the plate/beam centreline. However, the plate/beam attachment point is in fact offset from the beam centreline by an amount equal to half the beam width and this has an effect on the accuracy of the theoretical model, especially at high frequencies where the cross sectional dimensions of the plate/beam junction are not negligible compared with the bending wavelength. Overall, the experimental results for the present example are reasonably well predicted by the theoretical model. The CLF of a uniform plate/uniform plate coupled structure (as for the coupled periodic structure but with the beams removed) is also shown in Figure 12 for comparison. As expected, the removal of the beams eliminates the band pass nature of the system and increases the CLF.

5. CONCLUSIONS

A method for evaluating the CLF of a plate with periodic stiffeners coupled to a uniform plate has been presented. The method is based on travelling wave analysis and takes into account the band pass nature of the plate with periodic stiffeners. To verify the formulation of the CLF, an experimental program was conducted to measure the internal loss factors of the structural elements *in situ*, as well as the CLF. The experimental procedure has been validated by comparing the internal loss factors measured *in situ* against the benchmark results obtained from measurements of the individual elements using the steady state power balance method. Experimental results of the CLF show reasonable agreement with the theoretical prediction and it is therefore suggested that the present formulation of CLF for a coupled periodic structure may be used for SEA studies.

However, it should be noted that the present study has only considered bending waves to simplify the analysis. In reality, in-plane waves are often generated at structural junctions and this may have a significant effect on wave transmission, particularly in situations where the frequency of interest is high or the plate thickness is large. The method of analysis presented in this paper may be of use for guiding the direction of further studies on coupled periodic structures involving in-plane waves.

REFERENCES

1. L. Brillouin 1946 *Wave Propagation in Periodic Structures*. New York: Dover.
2. D. J. Mead 1971 *Transaction of the American Society of Mechanical Engineers*, *Journal of Engineering for Industry* **93**, 783–792. Vibration response and wave propagation in periodic structures.
3. M. Heckl 1964 *Journal of the Acoustical Society of America* **36**, 1335–1343. Investigation on the vibration of grillages and other simple beam structures.
4. D. J. Mead and N. S. Bardell 1986 *Journal of Sound and Vibration* **111**, 229–250. Free vibration of a cylindrical shell with discrete axial stiffeners.
5. D. J. Mead and N. S. Bardell 1987 *Journal of Sound and Vibration* **115**, 499–520. Free vibration of a thin cylindrical shell with periodic circumferential stiffeners.
6. R. S. Langley 1991 *Journal of Sound and Vibration* **145**, 261–277. An elastic wave technique for the free vibration of plate assemblies.
7. A. J. Keane and W. G. Price 1989 *Proceedings of the Royal Society of London*, *Series A* **423**, 332–360. Statistical energy analysis of periodic structures.
8. L. Cremer, M. Heckl and E. E. Ungar 1988 *Structure-borne Sound*. Berlin: Springer.

9. R. S. Langley 1994 *Journal of Sound and Vibration* **174**, 491–511. On the modal density and energy flow characteristics of periodic structures.
10. F. J. Fahy and A. D. Mohammed 1992 *Journal of Sound and Vibration* **158**, 45–67. A study of uncertainty in applications of SEA to coupled beam and plate systems, part I: computational experiments.
11. D. A. Bies and S. Hamid 1980 *Journal of Sound and Vibration* **70**, 187–204. *In situ* determination of loss and coupling loss factors by the power injection method.
12. R. H. Lyon and R. G. DeJong 1995 *Theory and Application of Statistical Energy Analysis*. London: Butterworth-Heinemann.
13. B. L. Clarkson and M. F. Ranky 1984 *Journal of Sound and Vibration* **94**, 249–261. On the measurement of the coupling loss factor of structural connections.

APPENDIX: WAVE TRANSMISSION ANALYSIS OF A PLATE WITH PERIODIC STIFFENERS

For a plate with periodic stiffeners of infinite extent as shown in Figure 1, the out-of-plane displacement of the plate at an arbitrary bay n is given by:

$$w(x_n) = \exp(\lambda_n)\left\{\sum_{m=1}^{4} A_m \exp(k_{mx}x_n)\right\}\exp(k_y y + \mathrm{j}\omega t), \tag{A1}$$

where l is the stiffener spacing, n is the element or bay number ($n = 0, 1, 2, \ldots, \infty$), $x_n = x - nl$, λ is the propagation constant, k_{mx} is the root of the dispersion equation for plate bending and A_m is the wave amplitude. If the plate is subjected to an oblique bending wave of wave number k_B and wave angle β, then k_{mx} and k_y may be expressed as [8]:

$$k_{1x} = \mathrm{j}k_B\cos\beta, \qquad k_{2x} = -\mathrm{j}k_B\cos\beta, \qquad k_{3x} = k_B\sqrt{[1+\sin^2\beta]},$$
$$k_{4x} = -k_B\sqrt{[1+\sin^2\beta]};$$

and $k_y = \pm\mathrm{j}k_B\sin\beta$.

Consider an arbitrary junction of the periodic structure as shown in Figure A1, the forces and displacements on the left-hand side of element n are related to the corresponding forces and displacements of element $n+1$ by the Bloch theorem as:

$$\exp(\lambda)w(x_n)|_{x_n=0} = w(x_{n+1})|_{x_{n+1}=0}, \tag{A2}$$

$$\exp(\lambda)\phi(x_n)|_{x_n=0} = \phi(x_{n+1})|_{x_{n+1}=0}, \tag{A3}$$

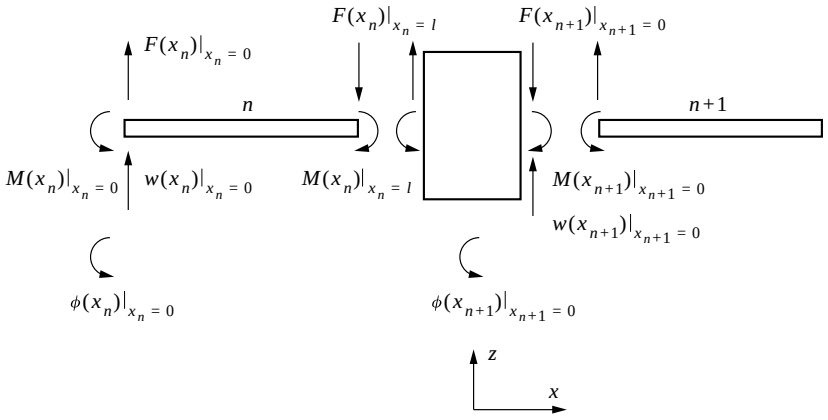

Figure A1. Forces and displacements at an arbitrary junction of a plate with periodic beam stiffeners.

$$\exp(\lambda)F(x_n)|_{x_n=0} = F(x_{n+1})|_{x_{n+1}=0}, \tag{A4}$$

$$\exp(\lambda)M(x_n)|_{x_n=0} = M(x_{n+1})|_{x_{n+1}=0}, \tag{A5}$$

where ϕ, F and M are the plate rotation, junction force and junction moment respectively. These quantities may be expressed in terms of the displacement $w(x_n)$ as:

$$\phi(x_n) = \partial w(x_n)/\partial x_n, \tag{A6}$$

$$F(x_n) = D[\partial^3 w(x_n)/\partial x_n^3 + (2-\mu)\partial^3 w(x_n)/\partial x_n \partial y^2], \tag{A7}$$

$$M(x_n) = -D[\partial^2 w(x_n)/\partial x_n^2 + \mu\partial^2 w(x_n)/\partial y^2], \tag{A8}$$

where D and μ are the flexural rigidity and Poisson's ratio of the plate elements respectively.

The right-hand side of equations (A2)–(A5) can be expressed in terms of element n by the compatibility and equilibrium requirements at the junction. Consider first the compatibility requirements:

$$w(x_{n+1})|_{x_{n+1}=0} = w(x_n)|_{x_n=l}, \tag{A9}$$

$$\phi(x_{n+1})|_{x_{n+1}=0} = \phi(x_n)|_{x_n=l}. \tag{A10}$$

The equilibrium of forces and moments at the junction must allow for the torsional, bending and inertia effects of the beam. As a result of beam bending in the y–z plane, the plate force F is augmented by the shear force of the beam. Summation of forces in the z-direction gives:

$$F(x_n)|_{x_n=l} - F(x_{n+1})|_{x_{n+1}=0} - \partial F_b/\partial y = -\rho A\omega^2 w(x_n)|_{x_n=l}, \tag{A11}$$

where $\partial F_b/\partial y = EI_x\partial^4 w(x_n)/\partial y^4|_{x_n=l}$, and ρ, A, E, I_x are the density, cross sectional area, elastic modulus and second moment of area of the beam respectively.

The variation in plate rotation along the y-axis causes the beam to twist and result in a torsional moment. Consider the equilibrium of moment about a line parallel to the y-axis and passing through the beam centroid:

$$M(x_n)|_{x_n=l} - M(x_{n+1})|_{x_{n+1}=0} - \partial M_b/\partial y = -I_c\omega^2\phi(x_n)|_{x_n=l}, \tag{A12}$$

where $\partial M_b/\partial y = -GJ\partial^2\phi(x_n)/\partial y^2|_{x_n=l}$, and G, J, I_c are the shear modulus, torsional constant and second moment of inertia per unit length of the beam respectively.

Eliminating the quantities that relate to element $n+1$ and expressing $w(x_n)$, $\phi(x_n)$, $F(x_n)$ and $M(x_n)$ in terms of the wave amplitudes $A_1, \ldots, A_4$ gives:

$$\sum_{m=1}^{4} A_m \exp(k_{mx}l) = \exp(\lambda)\sum_{m=1}^{4} A_m, \tag{A13}$$

$$\sum_{m=1}^{4} A_m k_{mx} \exp(k_{mx}l) = \exp(\lambda)\sum_{m=1}^{4} A_m k_{mx}, \tag{A14}$$

$$\sum_{m=1}^{4} (k_{mx}^2 - I_c\omega^2 k_{mx}/D - GJk_y^2 k_{mx}/D + \mu k_y^2)A_m \exp(k_{mx}l) = \exp(\lambda)\sum_{m=1}^{4} (k_{mx}^2 + \mu k_y^2)A_m, \tag{A15}$$

$$\sum_{m=1}^{4} (k_{mx}^3 + \rho A\omega^2/D - EI_x k_y^4/D + (2-\mu)k_y^2 k_{mx})A_m \exp(k_{mx} l)$$

$$= \exp(\lambda) \sum_{m=1}^{4} (k_{mx}^3 + (2-\mu)k_y^2 k_{mx})A_m. \tag{A16}$$

Equations (A13)–(A16) can be expressed in matrix form:

$$\mathbf{\Lambda}[A_m] = \exp(\lambda)[A_m], \tag{A17}$$

where $\mathbf{\Lambda}$ is a 4×4 matrix and $[A_m]$ is a column vector.